1000-0569/2016/032(11)-3269-80 *Acta Petrologica Sinica* 岩石学报

右江盆地酸性脉岩继承锆石成因及地质意义*

朱经经[1] 钟宏[1] 谢桂青[2] 赵成海[1] 胥磊落[1] 陆刚[3]

ZHU JingJing[1], ZHONG Hong[1], XIE GuiQing[2], ZHAO ChengHai[1], XU LeiLuo[1] and LU Gang[3]

1. 中国科学院地球化学研究所,矿床地球化学国家重点实验室,贵阳 550081
2. 中国地质科学院矿产资源研究所,国土资源部成矿作用与资源评价重点实验室,北京 100037
3. 广西壮族自治区区域地质调查研究院,桂林 541003

1. *State Key Laboratory of Ore Deposits Geochemistry, Institute of Geochemistry, Chinese Academy of Sciences, Guiyang* 550081, *China*
2. *MLR Key Laboratory of Metallogeny and Mineral Assessment, Institute of Mineral Resources, Chinese Academy of Geological Sciences, Beijing* 100037, *China*
3. *Institute of Regional Geological Survey of Guangxi Zhuang Autonomous Region, Guilin* 541003, *China*

2016-04-30 收稿, 2016-08-20 改回.

Zhu JJ, Zhong H, Xie GQ, Zhao CH, Xu LL and Lu G. 2016. Origin and geological implication of the inherited zircon from felsic dykes, Youjiang basin, China. *Acta Petrologica Sinica*, 32(11):3269-3280

Abstract The relationship between the Carlin-type gold deposits with magmatism is still debatable. Numerous Carlin-type gold deposits occur in the Youjiang basin, Southwest China. Due to the limited exposures of magmatic rocks within this region, it is unknown if there is genetic connections between magmatism and gold mineralization. The inherited zircons found in igneous rocks could give insight into the older or hidden magmatic events which are poorly exposed at the surface. The Bama, Liaotun, and Xiabaha quartz porphyry dykes host plenty of inherited zircons, among which the Liaotun and Xiabaha dykes are spatially present within the Liaotun and Mingshan gold deposits, respectively. Five main age clusters at 130 ~ 140Ma, ca. 242Ma, 400 ~ 450Ma, 700 ~ 1000Ma, and 1700 ~ 1800Ma were recognized in the inherited zircons by both LA-ICP-MS and SIMS U-Pb dating. The two younger groups of inherited zircons from the Liaotun and Xiabaha dykes give concordant U-Pb ages of 136.3 ± 3.9Ma (2σ), 242.3 ± 1.7Ma (2σ) and 128.2 ± 2.3Ma (2σ), 243.1 ± 3.6Ma (2σ), respectively. All the three dykes intruded the strata including the Middle Triassic Baifeng Formation (Member 1 and 2; 247 ~ 244Ma) and older sequences. Therefore, those zircons with ages older than the Middle Triassic should be probably captured from the host sedimentary rocks. Conversely, those at 130 ~ 140Ma might be derived from the hidden magmatic intrusions. For the zircons at ca. 242Ma, though coeval to the first and second members of the Baifeng Formation, they usually occur as anhedral fractions, indicating they might be inherited from the detrital zircons hosted by the sandstone and siltstone of the Baifeng Formation. Combined with the regional magmatism and geological setting, we propose that the ages of Triassic zircon forming events could represent the magmatic pulse related to the closure of the Paleo-Tethys Ocean. The zircon ages of 130 ~ 140Ma and ca. 242Ma are generally consistent with the timing of gold mineralization in the Youjiang basin. Thus, we prefer that there might be genetic links between magmatism and the formation of Carlin-type gold deposits in the Youjiang basin.

Key words Youjiang basin; Carlin-type gold deposits; Inherited zircon; Zircon U-Pb dating

摘 要 卡林型金矿与岩浆作用的关系一直以来是矿床学家关注的热点。右江盆地发育众多卡林型金矿床,但由于区内岩浆岩出露十分有限,岩浆活动对金成矿有无贡献目前还无定论。火成岩中的继承锆石常常可以用来指示早期的、隐伏的岩浆活动。桂西北地区晚白垩世巴马、料屯和下巴哈石英斑岩脉中含有大量的继承锆石。其中,料屯和下巴哈两处脉岩分别与料屯和明山金矿在空间上紧密相关。脉岩中锆石的 LA-ICP-MS 和 SIMS 原位 U-Pb 定年表明,其主要集中于 130 ~ 140Ma、

* 本文受国家"973"项目(2014CB440902)、国家自然科学基金项目(41230316、41303040)、中国科学院-国家外专局国际合作伙伴计划项目(KZZD-EW-TZ-20)联合资助.

第一作者简介:朱经经,男,1985 年生,博士,副研究员,主要从事矿床地球化学和岩石地球化学的研究工作,E-mail: zhujingjing@vip.gyig.ac.cn

242Ma 左右、400 ~ 450Ma、700 ~ 1000Ma 和 1700 ~ 1800Ma 等五个年龄段。关于较年轻的两个时间段,来自料屯和下巴哈石英斑岩脉的继承锆石分别获得两组谐和年龄,即 136.3 ± 3.9Ma(2σ) 和 242.3 ± 1.7Ma(2σ)、128.2 ± 2.3Ma(2σ) 和 243.1 ± 3.6Ma(2σ)。这些脉岩侵入的最年轻地层为中三叠统百逢组,因而前三叠纪继承锆石可能捕获自地层,而晚于三叠纪的 130 ~ 140Ma 锆石则应来自于深部隐伏岩体。关于 242Ma 左右锆石,尽管其与围岩地层百逢组 1 ~ 2 段近于同期,但其晶形较差且多呈不规则碎片状,暗示其更可能源自百逢组中的沉积碎屑锆石。结合区域地质背景,认为该期锆石所代表的岩浆事件可能与古特提斯洋闭合有关。以上 130 ~ 140Ma 和约 242Ma 左右的两组年龄,与初步确定的右江盆地卡林型金矿的两次成矿的时代基本一致,据此推断金矿化与岩浆作用可能有一定成因联系。

关键词 右江盆地; 卡林型金矿; 继承锆石; 锆石 U-Pb 定年

中图法分类号 P588.132; P597.3

1 引言

卡林型金矿是一种沉积岩容矿的微细浸染型金矿床,在全球该类型矿床主要分布于美国内华达州北部地区和我国的右江盆地及西秦岭地区(Hu *et al.*, 2002; Zhang *et al.*, 2003; Cline *et al.*, 2005; Kesler *et al.*, 2005; Peters *et al.*, 2007; Su *et al.*, 2008, 2009a, 2012; Hu and Zhou, 2012)。近年来的研究表明,美国内华达的卡林型金矿主要形成于 33 ~ 42Ma(Tretbar *et al.*, 2000; Cline, 2001; Arehart *et al.*, 2003),与区内始新世大规模岩浆活动具有一定的成因联系(Henry and Boden, 1998; Ressel *et al.*, 2000; Ressel and Henry, 2006; Muntean *et al.*, 2011; Johnson *et al.*, 2015)。我国右江盆地发育的卡林型金矿与美国内华达州具有很多相似性,但其形成时代和成矿机理(包括硫、金及成矿流体的来源等)却远未得到有效约束。成矿时代方面,前人针对各类矿物采用了多种定年方法,给出了十分宽泛的年龄范围: 36 ~ 267Ma(Hu *et al.*, 2002; 胡瑞忠等,2007a; Su *et al.*, 2009b; Chen *et al.*, 2015)。其中,如下两组年龄可能相对集中: (1) 通过方解石 Sm-Nd 同位素定年,获得了数个卡林型金矿的成矿时代可能为 135 ~ 150Ma(Su *et al.*, 2009b; 王泽鹏, 2013); (2) 含砷黄铁矿、毒砂 Re-Os 及云母 $^{40}Ar/^{39}Ar$ 和蚀变成因金红石 U-Pb 定年结果表明,金成矿时代可能为 200 ~ 230Ma 左右(陈懋弘等,2007,2009; Chen *et al.*, 2015)。成矿机理方面,不少学者提出岩浆作用对金成矿十分关键(黄永全和崔永勤,2001; 刘建中等,2006; 王泽鹏,2013)。然而,除与峨眉山地幔柱有关的基性侵入体外(260Ma; Xu *et al.*, 2008),右江盆地内部火成岩出露十分有限; 现有的研究表明,区内发育的少量超基性和酸性脉岩主要形成于 80 ~ 100Ma(Liu *et al.*, 2010c; 陈懋弘等,2012,2014),较上述两组成矿年龄明显年轻,且部分矿区发现脉岩切穿金矿体的地质现象(陈懋弘等,2014)。因而,很难将卡林型金矿与已出露的岩浆活动联系起来。然而,就区内是否存在隐伏岩体及其与金成矿是否存在成因联系等科学问题,目前尚不明确。

作者的初步研究显示,上述晚白垩世酸性脉岩往往富含大量的继承锆石。尽管继承锆石的来源十分复杂,但依然可能为早期的、隐伏的岩浆活动带来一些指示(Hoskin and Schaltegger, 2003; Pereira *et al.*, 2011)。因而,对这些继承锆石进行深入研究,可能会为我们评估岩浆作用对金成矿的贡献提供有益的线索。本文选取右江盆地出露的三处酸性脉岩(其中两处与金矿床具紧密的空间联系)中的继承锆石为研究对象,通过锆石 U-Pb 定年手段,提取区内隐伏的岩浆岩信息并分析其构造意义,进而探究岩浆活动与卡林型金矿是否存在成因联系。

2 地质背景

右江盆地位于扬子克拉通(其与华夏陆块共同组成华南板块)的西南缘,并以哀牢山-红河断裂与西南侧的三江古特提斯构造域相连(图 1; Peters *et al.*, 2007; Hu and Zhou, 2012)。盆地南侧与越北陆块为邻,二者可能被另一条古特提斯洋缝合带(即滇琼缝合带,图 1a, Cai and Zhang, 2009; Yang *et al.*, 2012a)隔开。连同师宗-弥勒断裂、凭祥-南宁断裂和紫云-亚都断裂,右江盆地被限制在一个近三角形的区域,故该区又被成为滇黔桂"金三角"。一般认为,早古生代晚期,伴随着古特提斯洋的打开,本区发生裂解并形成裂谷盆地,同时接受了大量浅水相的碳酸盐岩沉积(Liu *et al.*, 2002; 杜远生等,2013)。至中三叠世,由于古特提斯洋的闭合,该区演变为前陆盆地,并发育以砂岩和泥岩为代表的深水浊流相沉积(Enos *et al.*, 2006)。详细的镜下鉴定表明,该套沉积岩中含有大量的火山碎屑物质(Yang *et al.*, 2012b)。值得指出的是,盆地西北侧发育中三叠世碳酸盐岩,表明该区域当时水深相对较浅(图 1)。

已有研究表明,右江盆地卡林型金矿的主要容矿岩石为晚古生代碳酸盐岩和中三叠统沉积碎屑岩,少部分为辉绿岩(Hu *et al.*, 2002; Peters *et al.*, 2007; Su *et al.*, 2009a; Goldfarb *et al.*, 2014)。从矿体形态上区分,碳酸盐岩容矿的金矿床往往发育层状矿体(如水银洞金矿),而碎屑岩容矿金矿床的矿体则主要受高角度断层控制,其中以烂泥沟超大型金矿床最为著名(Zhang *et al.*, 2003; Xia *et al.*, 2012)。尽管容矿岩石和矿体产状不尽相同,但各卡林型金矿具有相似的矿物组合、矿床地球化学特征,暗示可能具有相似的成因机制(Hu *et al.*, 2002; Zhang *et al.*, 2003; Peters *et al.*, 2007)。盆地内部构造活动强烈,并以北东和北西向断层最

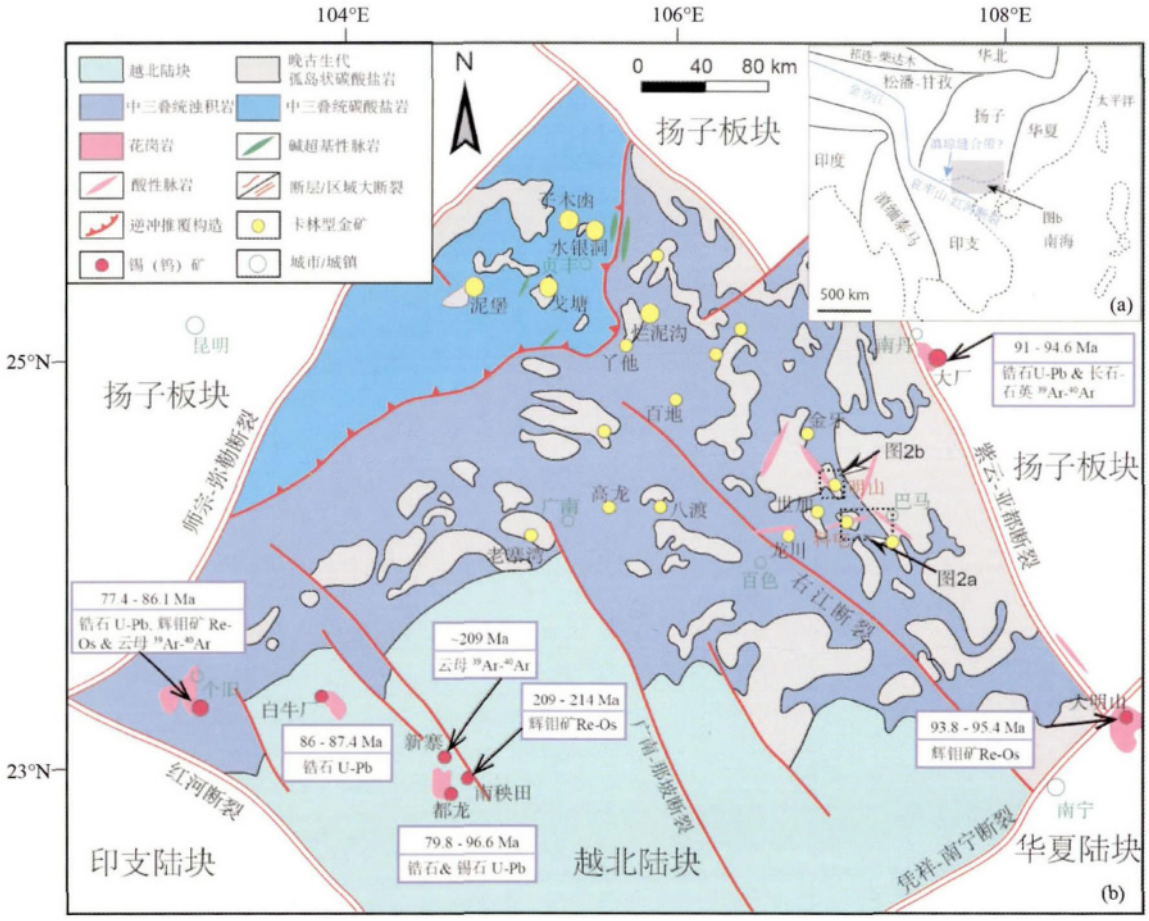

图 1　右江盆地构造位置(a) 及其地质简图(b) (据 Cai and Zhang，2009; Hou *et al.* ，2016 修改)

图中各 Sn(W) 矿床的年龄数据来源于文献汇总(Wang *et al.* ，2004; 李水如等，2008; 冯佳睿等，2011; Cheng *et al.* ，2013; Mao *et al.* ，2013; Xu *et al.* ，2015)

Fig. 1　Tectonic framework of the Youjiang basin (a) and its simplified geologic map (b) showing the distribution of Carlin-type gold deposits and igneous intrusions in the basin (modified after Cai and Zhang，2009; Hou *et al.* ，2016)

Ages for the Sn (W) deposits are summarized from Wang *et al.* ，2004; Li *et al.* ，2008; Feng *et al.* ，2011; Cheng *et al.* ，2013; Mao *et al.* ，2013; Xu *et al.* ，2015

为发育，其中北西向右江大断裂可能控制了区内大多数金矿床的展布(图 1b; Peters *et al.* ，2007) 。具体而言，这些矿床主要发育于背斜的两翼或受控于次级断裂(Hu *et al.* ，2002; Zhang *et al.* ，2003; Su *et al.* ，2009a; Xia *et al.* ，2014) 。

前已述及，除与峨眉山地幔柱相关的辉绿岩侵入体略显规模外，区内岩浆岩仅零星出露。在盆地北部出露一些碱性的超基性岩脉，该组岩脉距卡林型金矿床约 30km(Su *et al.* ，2009b) ，锆石 U-Pb 定年结果显示其形成于 85 ~ 88Ma(Liu *et al.* ，2010c) 。而在盆地的西侧，发育一系列沿北西和北东断裂分布的酸性脉岩。少量的定年结果显示，这些脉岩主要形成于 90 ~ 100Ma(陈懋弘等，2012，2014) 。此外，在盆地的南部和西部边缘，出露一些晚白垩世大型花岗岩侵入体，并产出一系列大型-超大型锡矿床(如个旧、大厂锡矿床，图 1b; Wang *et al.* ，2004; Hu and Zhou，2012; Cheng *et al.* ，2013; Mao *et al.* ，2013; Xu *et al.* ，2015) 。

3　样品与岩石学特征

右江盆地的酸性脉岩主要出露于桂西北地区，其中大部分分布于卡林型金矿的外围(陈懋弘等，2012) ，少部分与金矿床在空间上紧密相关。脉岩一般沿北东向和北西向断裂分布，倾角较陡。脉体宽度一般不超过 20m，而走向上可延伸至 20km。本文选取三处酸性脉岩开展研究，其中料屯和下巴哈两处脉岩分别横穿料屯和明山金矿矿区，而巴马脉岩与金矿床无直接空间联系(图 2) 。

料屯脉岩沿龙田背斜核部发育的北东向断裂产出，倾角近乎直立。围岩地层有石炭系、二叠系灰岩及中三叠统百逢组砂岩-泥岩(属百逢组 1 ~ 2 段，图 2a) 。该脉岩沿走向上延伸约 10km，脉宽 10m 左右。采样点远离料屯金矿区，该处脉岩侵入至下二叠统灰岩地层中。岩石呈灰白色，斑状结构，

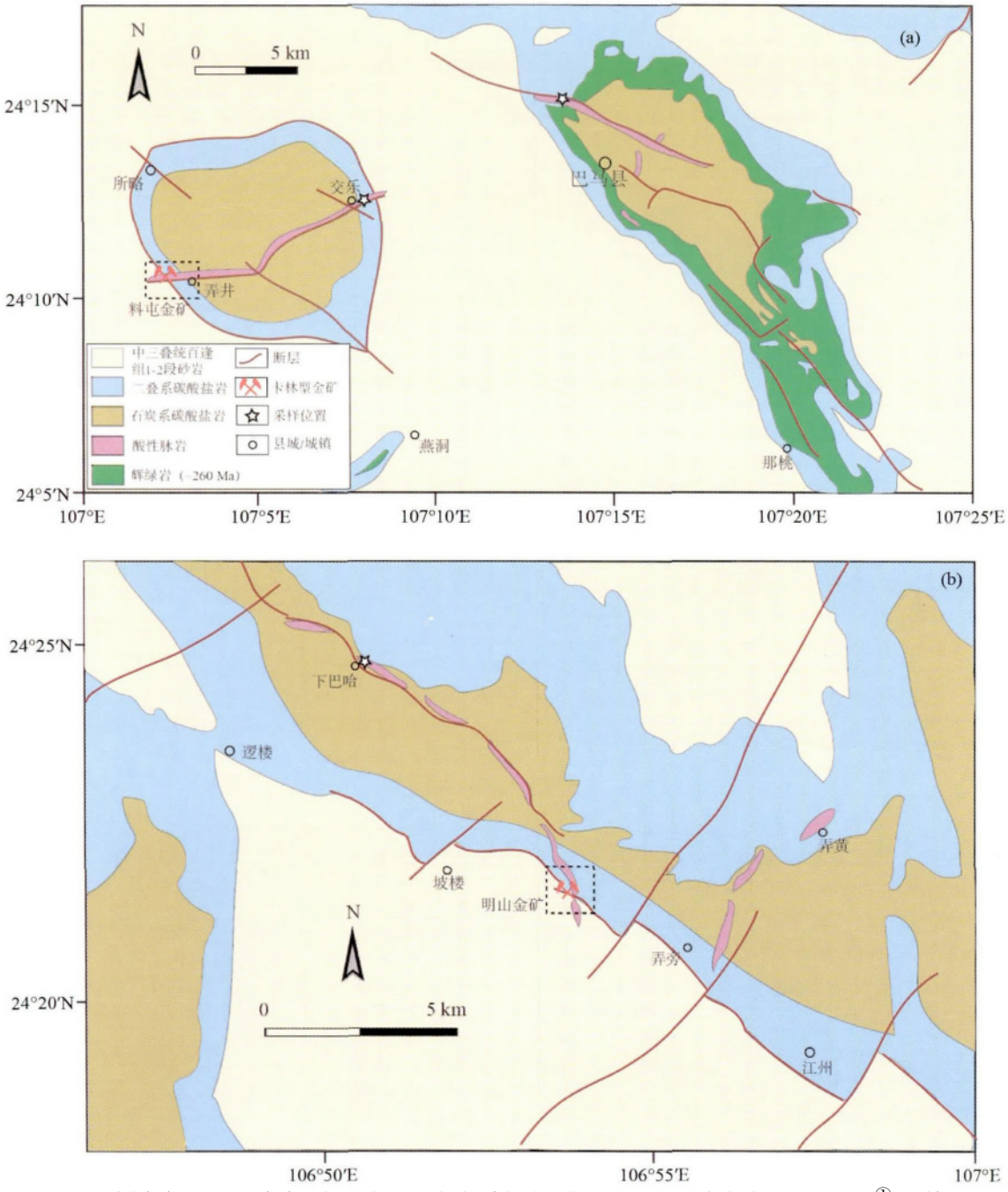

图 2 巴马、料屯(a)和下巴哈(b)酸性脉岩分布地质图(据广西壮族自治区区域地质测量队,1971①修编)

Fig. 2 Geological distribution of the Bama, Liaotun (a), and Xiabaha (b) felsic dykes

其中斑晶主要为石英和白云母,粒径为 0.2 ~ 2mm,含量约占 10%;基质以石英、白云母和碱性长石为主,岩石学上可定名为石英斑岩(图 3a)。地球化学研究表明,料屯酸性脉岩富集硅(SiO_2 质量分数为 75% ~ 80%)和钾,属于过铝质 S 型花岗岩(李院强等,2014)。料屯金矿矿区内,矿体主要赋存于百逢组第 2 段砂岩-泥岩地层中,走向北西。石英斑岩脉沿北东向断层侵入至百逢组地层,近脉岩处砂泥岩发育显著硅化,同时切穿金矿体,暗示金成矿早于脉岩的侵位(陈懋弘等,2014)。

下巴哈脉岩主要沿北西-北北西向断裂相间出露,倾角为 60° ~ 80°,脉宽约 4m。其西北段主要侵入至石炭系碳酸盐岩地层中,向东南延伸约 10km,且围岩逐渐过渡到二叠系

① 广西壮族自治区区域地质测量队. 1971. 东兰幅(G-48-XXXVI)1∶20 万矿产图和田林幅(G-48-XXXV)1∶20 万地质图

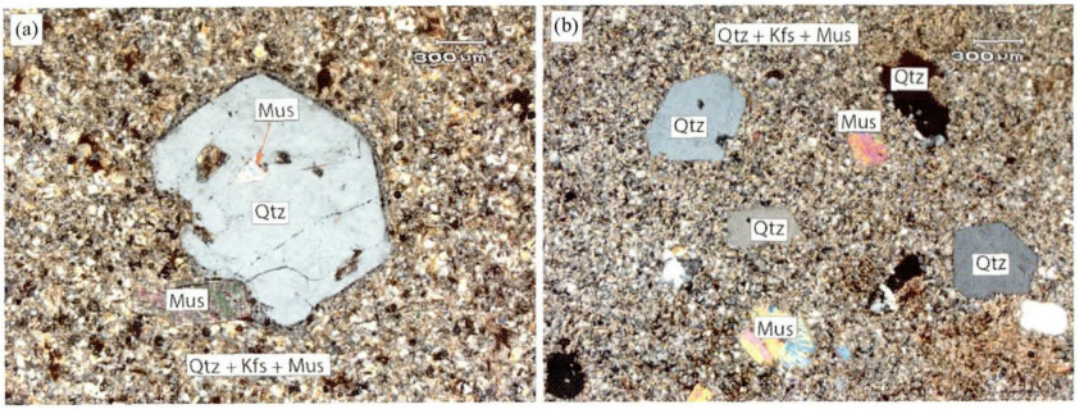

图 3 料屯(a)和巴马(b)酸性脉岩显微照片(正交偏光)

矿物缩写: Kfs-钾长石; Mus-白云母; Qtz-石英

Fig. 3 Representative transmitted photomicrographs of the Liaotun (a) and Bama (b) felsic dykes (cross-polarized light)

Abbreviations: Kfs-potassium feldspar; Mus-muscovite; Qtz-quartz

灰岩及中三叠统百逢组 1 ~ 2 段砂岩-泥岩地层(图 2b)。采样点位于该脉岩的西北段。与料屯石英斑岩脉相比,二者具有相似的地球化学特征(黄永全和崔永勤,2001);岩石学方面,斑晶以石英为主,白云母相对较少。该系列脉岩的东南段横穿明山金矿区,并侵入至下二叠统茅口组和中三叠统百逢组地层中(黄永全和崔永勤,2001; 庞保成等,2014)。金矿体主要受近东西向断裂控制,赋存于百逢组第 2 段砂泥岩地层中; 尽管未见脉岩与矿体直接的穿切关系,但二者显著斜交,可能不具有成因联系(庞保成等,2014)。

巴马酸性脉岩沿巴马背斜核部发育的北西向断裂产出,倾角近直立,出露宽度 5 ~ 10m,走向上延伸近 10km。与料屯和下巴哈石英斑岩脉不同的是,围岩地层除石炭系和二叠系碳酸盐岩外,还包括晚二叠世辉绿岩(张晓静和肖加飞,2014);但未见脉岩侵入至中三叠世砂泥岩地层的地质现象(图 2a)。在采样点附近,该脉岩侵入至下二叠统灰岩地层中。岩石学方面,其与料屯石英斑岩脉相似,均为斑状结构,斑晶以石英和白云母为主,基质为石英、白云母和碱性长石(图 3b);地球化学特征亦与料屯和下巴哈脉岩基本一致(陈懋弘等,2012)。

4 锆石 U-Pb 定年方法

分别采集料屯、下巴哈和巴马石英脉岩约 20kg(采样点见图 2)。为保证样品纯度,首先剔除了表面风化层,随后送至廊坊诚信地质服务公司挑选锆石。巴马脉岩挑选出的锆石较多(超过 300 粒),以柱状自形晶为主,长度为 100 ~ 200μm,长宽比一般为 2∶1。料屯和下巴哈脉岩的锆石含量较少,分别仅挑出 50 粒左右,自形程度较差,少量可见长柱状晶形,多为锆石碎片。颗粒一般较小,长度不超过 100μm。为获得准确可靠的分析结果,基于上述锆石的不同形态特征,选取了不同的测试仪器和分析方法。

4.1 巴马酸性脉岩

选取代表性的锆石约 200 粒制作环氧树脂靶,并拍摄透射光和反射光显微照片,以查明锆石的内部结构。上述工作在北京锆年领航科技有限公司完成。由于锆石颗粒较大,选择激光剥蚀-电感耦合等离子质谱仪(LA-ICP-MS)开展锆石 U-Pb 定年工作。该项测试在中国科学院地球化学研究所矿床地球化学国家重点实验室完成,使用仪器为 193nm 型准分子激光剥蚀系统(型号: GeoLasPro)和 ELANDRC-e 电感耦合等离子体质谱。测试期间,激光束能量密度为 10J/cm^2,束斑直径为 32μm,频率为 5Hz,剥蚀时间为 40s。使用标准锆石 91500 矫正仪器质量歧视效应和元素分馏,而标准锆石 GJ-1 和 Plešovice 作为未知样,用以检验数据质量。单点分析的同位素比值及年龄误差为 1σ。ICPMSDataCal10.2 和 Isoplot 3.76 软件分别被用来处理原始数据和进行年龄计算(Liu *et al.*, 2010a; Ludwig, 2012)。测得的锆石 GJ-1 和 Plešovice 的^{206}Pb/^{238}U 加权平均年龄均与推荐值(GJ-1: ~ 599.8Ma, Liu *et al.*, 2010b; Plešovice: ~ 337.1Ma, Sláma *et al.*, 2008)在误差范围内一致。具体分析流程与 Liu *et al.* (2010a,b)的描述相同。

4.2 料屯和下巴哈酸性脉岩

将所有锆石样品并标样 TEM2(416.8Ma; Black *et al.*, 2004)和 6266(559.0Ma; Stern and Amelin, 2003)用以制作环氧树脂靶。为揭示锆石的内部结构,完成透-反射光显微照相后,将锆石靶表面镀金并拍摄扫描电镜(SEM)、阴极发光(CL)和背散射(BSE)图像。所用仪器为蔡司公司生产的 EVO MA15 扫描电镜,并配有宽频 CL 和 BSE 探头。鉴于锆石颗粒较小,选择离子探针质谱仪(SIMS: Cameca IMS 1280)开展锆石 U-Pb 同位素测试工作。用强度为 1nA 一次 O_2^- 离子束轰击样品表面(轰击能量: 23kV),束斑为 15μm × 18μm。

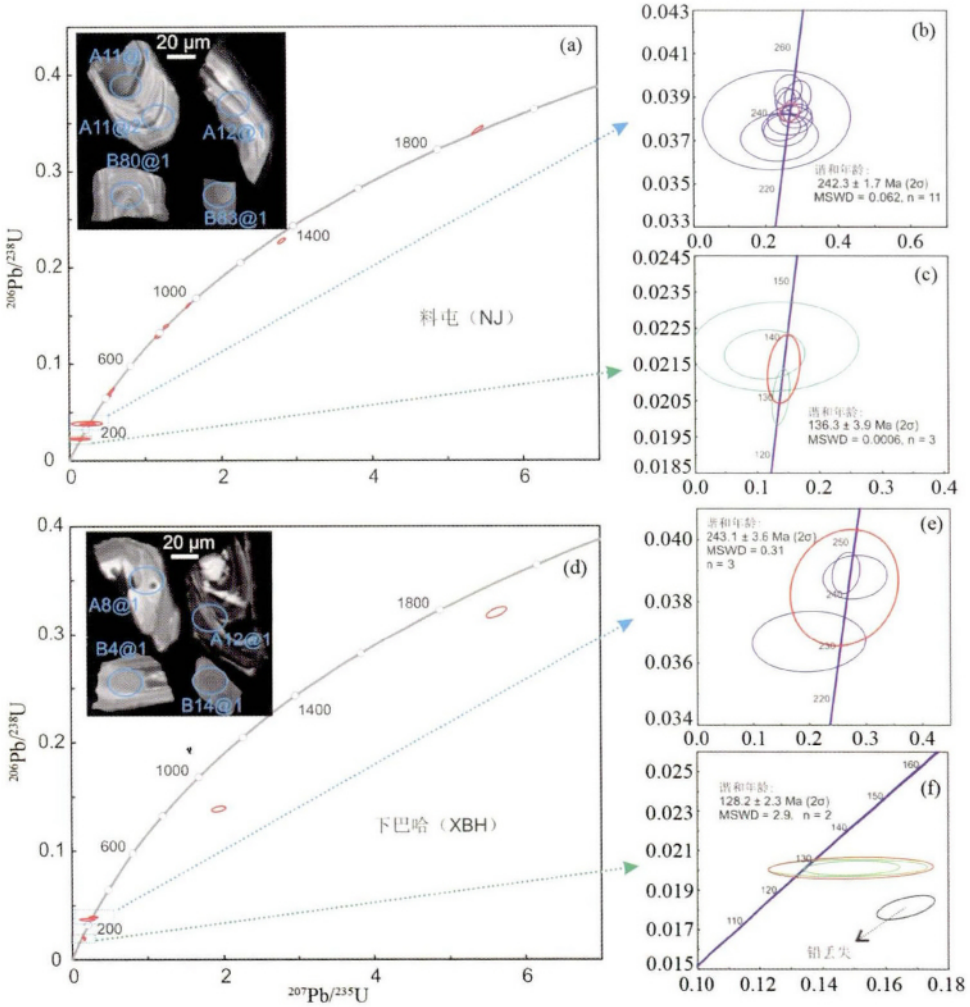

图 4 料屯(a-c)和下巴哈(d-f)酸性脉岩中继承锆石 U-Pb 谐和年龄图

图 a、d 展示了代表性锆石的阴极发光图片,其中红色椭圆代表分析点位,并附相应点号(表 2). 大部分锆石呈碎片状,且边部多由于溶蚀而呈不规则状;少量晶体较完整的锆石边部呈不规则状或浑圆状,暗示经历溶蚀或搬运、磨圆等沉积过程. 图 b、c 和 e、f 中的红色椭圆代表 ISOPLOT 软件计算的谐和年龄范围(Ludwig, 2012),分析点误差为 1σ

Fig. 4 Concordia diagrams of SIMS U-Pb isotopic analyses of inherited zircons for the Liaotun (a-c) and Xiabaha (d-f) felsic rocks

Cathodoluminescence images of representative inherited zircons with spot numbers (red ellipse) are included in Fig. 4a, d, corresponding to the spot analyses given in Table 2. Note most of the zircons occur as fractions with irregular edges, and the relatively euhedral crystals have irregular edges or round shapes, indicative of corrosion or sedimentary processes including transportation and rounding. The red ellipses reflect the concordia ages calculated by ISOPLOT (Ludwig, 2012) in Fig. 4b, c, e, f. Data-point error ellipses are 1σ

以上工作均在加拿大阿尔伯塔大学完成。用标准锆石 TEM2 校正样品的 Pb/U 比值,Th 和 U 含量则通过标准锆石 6266 计算获得,并基于实测^{204}Pb含量校正普通 Pb。单点分析的同位素比值及年龄误差为 1σ。原始数据处理采用 SQUID2 软件(Ludwig, 2009),并通过 ISOPLOT 3.76 软件计算谐和年龄(Ludwig, 2012)。标准锆石 6266 的$^{206}Pb/^{238}U$加权平均年龄为 560 ± 1.5Ma(MSWD = 2.4),与其推荐值在误差范围内一致。详细分析流程请见 Stern *et al.* (2009)。

5 锆石 U-Pb 年龄

除原生结晶锆石外,3 个酸性脉岩样品均富含数量不等的继承锆石。阴极发光图像显示大部分锆石都具有很好的岩浆环带(图 4a, d)。与结晶锆石相比,继承锆石晶形较差,多为锆石碎片,且边部形状不规则,可能暗示其遭受了不同程度的溶蚀;其他少量晶体较完整的锆石边部呈浑圆状或不规则状,暗示经历溶蚀或搬运、磨圆等沉积过程。原生结晶锆石的 U-Pb 年龄为 95 ~ 100Ma,与陈懋弘等(2012,2014)报道的白云母$^{40}Ar/^{39}Ar$年龄(95Ma 左右)在误差范围内一致。继承锆石年龄显著较老,其$^{206}Pb/^{238}U$表面年龄主要集中于 130 ~ 140Ma、242Ma 左右、400 ~ 450Ma、700 ~ 1000Ma 和 1700 ~ 1800Ma 等五个年龄段(图 5)。具体而言,各个脉岩中的继承锆石的特征和年龄略有不同。值得提出的是,由于前人

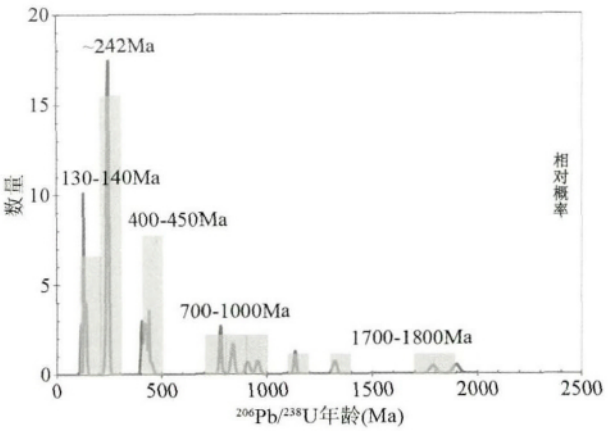

图 5 酸性脉岩中继承锆石的$^{206}Pb/^{238}U$模式年龄分布图

Fig. 5 Frequency of $^{206}Pb/^{238}U$ model ages of the inherited zircons

已对上述脉岩的成岩时代进行了有效约束(陈懋弘等,2012,2014),且本文的重点是通过继承锆石推测区内隐伏的岩浆活动并探讨其与金成矿的关系,因而对原生结晶锆石的U-Pb年龄不作深入讨论。

(1)巴马酸性岩脉。该脉岩样品(BM)中的锆石以结晶期岩浆锆石为主,继承锆石相对较少。对35个锆石颗粒进行了LA-ICP-MS U-Pb定年,其中仅5颗属于继承锆石(表1)。这些继承锆石的$U = 244 \times 10^{-6} \sim 2076 \times 10^{-6}$,$Th = 108 \times 10^{-6} \sim 898 \times 10^{-6}$,相应的$Th/U = 0.23 \sim 0.66$。$^{206}Pb/^{238}U$年龄主要分布于400~450Ma和700~1000Ma两个时间段。

(2)料屯酸性脉岩。该脉岩样品(NJ)含有大量的继承锆石,而结晶期岩浆锆石相对较少。其中,很多继承锆石的晶形不完整(图4a)。对样品NJ的27个锆石颗粒进行了SIMS U-Pb同位素分析,其中继承锆石为24颗(表2)。这些锆石的Th和U含量变化较大($U = 91.4 \times 10^{-6} \sim 1410 \times 10^{-6}$,$Th = 39.6 \times 10^{-6} \sim 448 \times 10^{-6}$),但Th/U相对一致,除分析点NJ-B82@1和NJ-A10@1之外,所有分析点的Th/U均大于0.1(0.13~1.21)。U-Pb年龄涵盖上述五个分布区间(图4a)。$^{206}Pb/^{238}U$年龄分布于242Ma左右和130~140Ma两个区间的锆石分别具有谐和的U-Pb同位素组成,与前者有关的11个分析点获得的谐和年龄为242.3±1.7Ma(2σ,MSWD=0.062;图4b),而与后者相关的3个分析点得到的谐和年龄为136.3±3.9Ma(2σ,MSWD=0.0006;图4c)。

(3)下巴哈酸性脉岩。下巴哈石英脉岩样品(XBH)的锆石也以继承锆石为主。由于锆石颗粒很小,仅选出11颗做SIMS U-Pb同位素分析,其中8颗为继承锆石(表2)。这些继承锆石的$U = 169 \times 10^{-6} \sim 4032 \times 10^{-6}$,$Th = 36 \times 10^{-6} \sim 640 \times 10^{-6}$,除分析点XBH-A2@1和XBH-B5@1之外,Th/U比值均大于0.1(0.27~0.88)。U-Pb年龄分布范围较广,但集中于130~140Ma和242Ma左右两个时间段(图4d)。前者含3个分析点,剔除一个明显发生Pb丢失的锆石,两个分析点获得的谐和年龄为128.2±2.3Ma(2σ,MSWD=2.9;图4f);而后者包括的3个分析点得到的谐和年龄为243.1±3.6Ma(2σ,MSWD=0.31;图4e)。

6 讨论

6.1 继承锆石的成因

锆石包括原生岩浆、继承、变质、热液等多种成因类型(Hoskin and Schaltegger, 2003; 吴元保和郑永飞, 2004; Schaltegger, 2007; Yang *et al.*, 2014)。而火成岩中的继承锆石大致具有两种来源:(1)捕获自围岩沉积岩地层;(2)来自于深部隐伏岩体。前者来自于碎屑锆石,常可以用来指示沉积的物源、沉积时代的上限以及重建古地理环境等(Gehrels *et al.*, 2011; Thomas, 2011)。而后者则对指示隐伏岩浆事件的时代十分关键(Condie *et al.*, 2009; Pereira *et al.*, 2011)。

巴马、料屯和下巴哈酸性脉岩的形成时代为95~100Ma,围岩地层主要为晚古生代(C-T)碳酸盐岩和碎屑岩,均远远老于成岩时代(图2)。其中最年轻的围岩为中三叠统百逢组1~2段(T_2b_{1-2})。百逢组形成于三叠世安尼期,其1~2段的形成时代约为247~244Ma(Ovtcharova *et al.*, 2006; Chen and Stiller, 2007)。因而,244Ma可以作为围岩地层中所含碎屑锆石的年龄下限。故我们获得的400~450Ma、700~1000Ma和1700~1800Ma等三个较老年龄段的锆石,很可能来自于围岩地层,而较年轻的130~140Ma的锆石应当来自于隐伏岩体。至于242Ma左右的继承锆石,其在误差范围内与百逢组1~2段近于同期,故上述两种来源均有可能。进一步的分析表明,该期锆石多呈碎片状(图4),具完整晶形者较少。此外,尽管料屯和下巴哈脉岩中该期锆石较多,而对未侵入至百逢组地层的巴马而言(图2a),并未发现242Ma左右的继承锆石(表1)。因而我们认为,该期继承锆石更有可能捕获自围岩地层。

6.2 华南板块西南缘中三叠世岩浆事件及其动力学背景

巴马、料屯和下巴哈脉岩中继承锆石的年龄主要分布于上述五个时间段,其中前三叠纪的三组年龄与华南板块主要的岩浆事件时限基本一致(Wang *et al.*, 2012, 2013; Yang *et al.*, 2012a),暗示其可能与华南板块内部的各期岩浆事件相关。而130~140Ma的隐伏岩浆活动,则与华南板块140~125Ma时间段的岩石圈伸展较为吻合(毛景文等,2004; 胡瑞忠等,2007b),初步认为二者可能存在成因联系。

关于242Ma左右的继承锆石,由于其与最年轻的围岩地层(百逢组1~2段)近于同时代,结合岩层内部存在不少火山碎屑(Yang *et al.*, 2012a),表明岩浆与沉积事件相隔很短,也暗示沉积区域应紧邻242Ma左右(中三叠世)岩浆活动的中心。右江盆地南缘发育一些早-中三叠世的岩浆岩,尤以一系列火山岩的产出为代表(覃小峰等,2011; Yang *et al.*, 2012b)。这些岩浆岩很可能为242Ma左右继承锆石的

表 1 巴马石英斑岩脉中继承锆石 LA-ICP-MS U-Pb 同位素分析数据

Table 1 LA-ICP-MS U-Pb isotopic data on the inherited zircons of the Bama quartz porphyry dyke

测点号	Th	U	Th/U	$^{207}Pb/^{235}U$		$^{206}Pb/^{238}U$		ρ	$^{207}Pb/^{235}U$ 年龄		$^{206}Pb/^{238}U$ 年龄		谐和度
	($\times10^{-6}$)			比值	1σ	比值	1σ		Ma	1σ	Ma	1σ	
巴马石英斑岩脉(BM: N24°10′16.90″, E107°12′49.91″)													
BM-28@1	275	822	0.33	0.5722	0.0124	0.0651	0.0011	0.7714	459	8.0	406	6.6	87%
BM-01@1	898	2067	0.43	0.5416	0.0062	0.0705	0.0004	0.4838	439	4.1	439	2.4	99%
BM-23@1	118	502	0.23	1.1617	0.0145	0.1283	0.0008	0.4956	783	6.8	778	4.5	99%
BM-13@1	162	244	0.66	1.8391	0.0299	0.1514	0.0019	0.7612	1060	10.7	909	10.5	84%
BM-29@1	108	438	0.25	2.1113	0.0231	0.1927	0.0011	0.5082	1153	7.5	1136	5.8	98%

表 2 料屯和下巴哈石英斑岩脉中继承锆石 SIMS U-Pb 同位素分析数据

Table 2 SIMS U-Pb isotopic data on the inherited zircons of the Liaotun and Xiabaha quartz porphyry dykes

测点号	U	Th	Th/U	$^{207}Pb^*/^{206}Pb^*$		$^{207}Pb^*/^{235}U$		$^{206}Pb^*/^{238}U$		$^{206}Pb/^{238}$ 年龄	
	($\times10^{-6}$)			比值	%	比值	%	比值	%	Ma	1σ
料屯石英斑岩脉(NJ: N24°12′33.25″, E107°07′31.23″)											
NJ-B82@1	1409	71	0.05	0.0492	6.1	0.14	6.6	0.021	2.5	131	3
NJ-B35@1	168	120	0.72	0.0381	37.0	0.11	37.1	0.022	2.1	139	3
NJ-A5@1	145	83	0.57	0.0429	68.5	0.13	68.6	0.022	3.7	140	5
NJ-A12@1	180	71	0.39	0.0468	29.5	0.24	29.5	0.037	2.0	235	5
NJ-B21@1	278	335	1.21	0.0495	15.7	0.26	15.7	0.037	1.3	237	3
NJ-A11@1	349	181	0.52	0.0471	14.4	0.24	14.5	0.038	1.1	238	3
NJ-A7@1	460	341	0.74	0.0515	15.2	0.27	15.2	0.038	1.2	240	3
NJ-A4@1	91	118	1.29	0.0441	58.3	0.23	58.4	0.038	4.0	240	9
NJ-A7@2	383	204	0.53	0.0543	10.1	0.29	10.2	0.038	1.0	241	2
NJ-B36@1	414	223	0.54	0.0537	7.9	0.28	7.9	0.038	1.0	243	2
NJ-A11@2	390	206	0.53	0.0504	8.5	0.27	8.6	0.039	1.3	244	3
NJ-B46@1	415	224	0.54	0.0477	6.9	0.26	7.0	0.039	0.9	246	2
NJ-B51@1	325	100	0.31	0.0542	8.1	0.29	8.2	0.039	1.3	247	3
NJ-B80@1	487	267	0.55	0.0487	9.4	0.26	9.5	0.039	1.2	249	3
NJ-A9@1	408	182	0.45	0.0550	4.5	0.49	4.6	0.065	0.9	403	4
NJ-B88@1	467	140	0.30	0.0568	3.0	0.52	3.1	0.067	0.9	416	4
NJ-B17@1	732	342	0.47	0.0566	1.1	0.53	1.5	0.068	1.0	423	4
NJ-B43@1	758	813	1.07	0.0545	1.7	0.52	1.9	0.069	0.9	429	4
NJ-B24@1	1155	448	0.39	0.0561	2.1	0.56	3.1	0.072	2.3	449	10
NJ-B18@1	555	153	0.28	0.0661	2.0	1.17	2.2	0.128	0.9	778	7
NJ-B25@1	292	100	0.34	0.0666	1.3	1.27	1.6	0.139	0.9	837	7
NJ-B10@1	1081	141	0.13	0.0708	0.5	1.56	1.2	0.160	1.1	957	10
NJ-B29@1	831	353	0.43	0.0899	0.7	2.82	1.1	0.227	0.9	1319	10
NJ-A10@1	512	40	0.08	0.1147	0.3	5.41	1.0	0.342	0.9	1897	15
下巴哈石英斑岩脉(XBH: N24°24′08.27″, E106°51′43.27″)											
XBH-B5@1	4032	134	0.03	0.0666	3.0	0.17	3.7	0.018	2.2	116	3
XBH-A2@1	1257	36	0.03	0.0540	6.7	0.15	6.8	0.020	1.2	128	1
XBH-A12@1	784	209	0.27	0.0535	11.3	0.15	11.3	0.020	1.4	128	2
XBH-A4@1	169	53	0.31	0.0394	33.3	0.20	33.3	0.037	1.8	232	4
XBH-A8@1	264	100	0.38	0.0526	13.2	0.28	13.3	0.039	1.2	245	3
XBH-B14@1	912	640	0.70	0.0495	6.1	0.27	6.2	0.039	1.1	246	3
XBH-A9@1	408	125	0.31	0.1014	2.9	1.93	3.2	0.138	1.3	836	10
XBH-B13@1	183	160	0.88	0.1278	1.2	5.64	1.6	0.320	1.1	1789	17

注: U-Pb 同位素数据误差均为 1σ, 且已扣除普通铅

源岩。对于该期岩浆事件,存在两种可能动力学机制: (1) 与太平洋板块西向平板俯冲有关(Li and Li,2007; Carter and Clift,2008; Li *et al.*, 2012); (2) 受印支运动即印支板块与华南板块的相互作用控制(Zhou *et al.*, 2006; Wang *et al.*, 2013)。依照太平洋板块平板俯冲模型,右江盆地及其邻近区域应发育 210Ma 左右的岩浆活动,而 240 ~ 250Ma 的岩浆活动则应集中于华南板块的东南缘。显然,该模型无法解释上述中三叠世的岩浆事件。事实上,除南缘发育的火山活动之外,右江盆地周边也产出大量的早-中三叠世的火成岩。包括西侧的金沙江-哀牢山古特提斯带(Zhu *et al.*, 2011; Zi *et al.*, 2012; Lai *et al.*, 2014; Liu *et al.*, 2015)、越北地块(Roger *et al.*, 2012)等。系列地质、地球化学证据表明,介于印支板块和华南板块之间的古特提斯洋闭合于中三叠世(245Ma 左右)或略早,松玛缝合带(Roger *et al.*, 2012; Faure *et al.*, 2014; Lai *et al.*, 2014; Wang *et al.*, 2014)和/或介于右江盆地与越北地块之间的滇琼缝合带(Cai and Zhang, 2009)可能是古特提斯洋闭合后的残余(图 1)。因而,本研究涉及的 242Ma 左右的继承锆石所代表的岩浆事件可能与古特提斯洋的闭合紧密相关。

6.3 卡林型金矿与岩浆的可能关系

尽管目前就右江盆地卡林型金矿的成矿时代争议较大,但较多的年龄数据表明这些金矿很可能形成于 135 ~ 150Ma (Su *et al.*, 2009b; 王泽鹏,2013) 或 200 ~ 230Ma 左右(陈懋弘等,2007,2009; Chen *et al.*, 2015)。前者主要基于以下两点认识: (1) 金成矿与去碳酸盐化蚀变紧密相关; (2) 方解石为去碳酸盐化的产物,故认为方解石的 Sm-Nd 同位素年龄可以代表金成矿时代。200 ~ 230Ma 左右的年龄主要来自于 Re-Os 同位素定年,所用样品为含金毒砂和含砷黄铁矿(陈懋弘等,2009; Chen *et al.*, 2015)。最近,皮桥辉等(个人交流,2016)采用离子探针手段,对云南者桑金矿热液金红石进行了 U-Pb 定年,由于金红石与载金矿物——含砷黄铁矿具显著共生关系,推断者桑金矿形成于 213.6 ± 5.4Ma (MSWD = 0.95)。该年龄与含砷黄铁矿、毒砂 Re-Os 定年结果在误差范围内一致。这表明右江盆地的卡林型金矿的早期成矿年龄可能为晚三叠世。

由上述讨论可以发现,右江盆地及周缘可能存在年龄在 130 ~ 140Ma 左右和约 242Ma 的隐伏花岗岩体。这两个时代的深部花岗岩浆活动与右江盆地两期卡林型金矿的成矿作用时代基本一致。这种时代上的一致性可能暗示,卡林型金矿的形成可能与其深部的岩浆活动具有成因联系。值得指出的是,这种推论是初步的,还需要更多成岩成矿精确年代学以及成矿流体地球化学的深入研究。

7 结论

(1) LA-ICP-MS 和 SIMS 锆石 U-Pb 定年表明,继承锆石主要集中于 130 ~ 140Ma、242Ma 左右、400 ~ 450Ma、700 ~ 1000Ma 和 1700 ~ 1800Ma 等五个年龄段。对于较年轻的两个时间段,料屯和下巴哈石英斑岩脉捕获的继承锆石分别获得两组谐和年龄,分别为 136.3 ± 3.9Ma (2σ) 和 242.3 ± 1.7Ma (2σ)、128.2 ± 2.3Ma (2σ) 和 243.1 ± 3.6Ma (2σ)。

(2) 前三叠世继承锆石应来源于围岩地层; 130 ~ 140Ma 锆石可能捕获自深部隐伏岩体,而 242Ma 左右的锆石颗粒与中三叠统百逢组近于同时代,进一步研究表明其可能来自于百逢组中的沉积碎屑锆石,该期锆石所代表的岩浆事件可能与古特提斯洋闭合有关。

(3) 右江盆地及周缘可能存在年龄在 130 ~ 140Ma 左右和约 242Ma 的隐伏花岗岩体。这两个时代的深部花岗岩浆活动与右江盆地两期卡林型金矿的成矿作用时代基本一致。这种时代上的一致性可能暗示,卡林型金矿的形成可能与其深部的岩浆活动具有成因联系。

致谢 在野外考察过程中得到中国科学院地球化学研究所肖加飞研究员、蓝江波博士、黄勇硕士、张晓静硕士及广西区域地质调查研究院潘艺文工程师的帮助; 锆石 U-Pb 定年工作分别在中国科学院地球化学研究所戴智慧高级工程师和加拿大阿尔伯塔大学 Richard Stern 博士的协助下完成; 胡瑞忠研究员对研究工作和论文的写作给予了指导和帮助; 西北大学刘燊教授和另外一位匿名评阅人对文章初稿提出了许多建设性意见; 在此一并表示感谢!

References

Arehart GB, Chakurian AM, Tretbar DR, Christensen JN, McInnes BA and Donelick RA. 2003. Evaluation of radioisotope dating of Carlin-type deposits in the Great Basin, western North America, and implications for deposit genesis. Economic Geology, 98(2): 235 - 248

Black LP, Kamo SL, Allen CM, Davis DW, Aleinikoff JN, Valley JW, Mundil R, Campbell IH, Korsch RJ, Williams IS and Foudoulis C. 2004. Improved $^{206}Pb/^{238}U$ microprobe geochronology by the monitoring of a trace-element-related matrix effect; SHRIMP, ID-TIMS, ELA-ICP-MS and oxygen isotope documentation for a series of zircon standards. Chemical Geology, 205(1-2): 115 - 140

Cai JX and Zhang KJ. 2009. A new model for the Indochina and South China collision during the Late Permian to the Middle Triassic. Tectonophysics, 467(1 - 4): 35 - 43

Carter A and Clift PD. 2008. Was the Indosinian orogeny a Triassic mountain building or a thermotectonic reactivation event? Comptes Rendus Geoscience, 340(2 - 3): 83 - 93

Chen JH and Stiller F. 2007. The halobiid bivalve genus Enteropleura and a new species from the Middle Anisian of Guangxi, southern China. Acta Palaeontologica Polonica, 52(1): 53 - 61

Chen MH, Mao JW, Qu WJ, Wu LL, Uttley PJ, Norman T, Zheng JM and Qin YZ. 2007. Re-Os dating of arsenian pyrites form the Lannigou gold deposit, Zhenfeng, Guizhou Province, and its geological significances. Geological Reviews, 53(3): 371 - 382 (in Chinese with English abstract)

Chen MH, Huang QW, Hu Y, Chen ZY and Zhang W. 2009. Genetic types of phyllosilicate (micas) and its $^{39}Ar-^{40}Ar$ dating in Lannigou gold deposit, Guizhou Province, China. Acta Mineralogica Sinica, 29(3): 353 - 362 (in Chinese with English abstract)

Chen MH, Lu G and Li XH. 2012. Muscovite $^{40}Ar/^{39}Ar$ dating of the quartz porphyry veins from Northwest Guangxi, China, and its geological significance. Geological Journal of China Universities, 18(1): 106 – 116 (in Chinese with English abstract)

Chen MH, Zhang Y, Meng YY, Lu G and Liu SQ. 2014. Determination of upper limit of metallogenic epoch of Liaotun gold deposit in western Guangxi and its implications for chronology of Carlin-type gold deposits in Yunnan-Guizhou-Guangxi "golden triangle" area. Mineral Deposits, 33(1): 1 – 13 (in Chinese with English abstract)

Chen MH, Mao JW, Li C, Zhang ZQ and Dang Y. 2015. Re-Os isochron ages for arsenopyrite from Carlin-like gold deposits in the Yunnan-Guizhou-Guangxi "golden triangle", southwestern China. Ore Geology Reviews, 64: 316 – 327

Cheng YB, Mao JW and Spandler C. 2013. Petrogenesis and geodynamic implications of the Gejiu igneous complex in the western Cathaysia block, South China. Lithos, 175 – 176: 213 – 229

Cline JS. 2001. Timing of gold and arsenic sulfide mineral deposition at the Getchell Carlin-type gold deposit, north-central Nevada. Economic Geology, 96(1): 75 – 89

Cline JS, Hofstra AH, Muntean JL, Tosdal RM and Hickey KA. 2005. Carlin-type gold deposits in Nevada: Critical geologic characteristics and viable models. Economic Geology 100th anniversary volume: 451 – 484

Condie KC, Belousova E, Griffin WL and Sircombe KN. 2009. Granitoid events in space and time: Constraints from igneous and detrital zircon age spectra. Gondwana Research, 15(3 – 4): 228 – 242

Du YS, Huang H, Yang JH, Huang HW, Tao P, Huang ZQ, Hu LS and Xie CX. 2013. The basin translation from Late Paleozoic to Triassic of the Youjiang basin and its tectonic signification. Geological Review, 59(1): 1 – 11 (in Chinese with English abstract)

Enos P, Lehrmann DJ, Wei JY, Yu YY, Xiao JF, Chaikin DH, Minzoni M, Berry AK and Montgomery P. 2006. Triassic evolution of the Yangtze platform in Guizhou Province, People's Republic of China. Geological Society of America Special Papers, 417: 1 – 105

Faure M, Lepvrier C, Van Nguyen V, Van Vu T, Lin W and Chen ZC. 2014. The South China block-Indochina collision: Where, when, and how? Journal of Asian Earth Sciences, 79: 260 – 274

Feng JR, Mao JW, Pei RF and Li C. 2011. A tentative discussion on Indosinian ore-forming events in Laojunshan area of southeastern Yunnan: A case study of Xinzhai tin deposit and Nanyangtian tungsten deposit. Mineral Deposits, 30(1): 57 – 73 (in Chinese with English abstract)

Gehrels GE, Blakey R, Karlstrom KE, Timmons JM, Dickinson B and Pecha M. 2011. Detrital zircon U-Pb geochronology of Paleozoic strata in the Grand Canyon, Arizona. Lithosphere, 3(3): 183 – 200

Goldfarb RJ, Taylor RD, Collins GS, Goryachev NA and Orlandini OF. 2014. Phanerozoic continental growth and gold metallogeny of Asia. Gondwana Research, 25(1): 48 – 102

Henry CD and Boden DR. 1998. Eocene magmatism: The heat source for Carlin-type gold deposits of northern Nevada. Geology, 26(12): 1067 – 1070

Hoskin PWO and Schaltegger U. 2003. The composition of zircon and igneous and metamorphic petrogenesis. Reviews in Mineralogy and Geochemistry, 53(1): 27 – 62

Hou L, Peng HJ, Ding J, Zhang JR, Zhu SB, Wu SY, Wu Y and Ouyang HG. 2016. Textures and in situ chemical and isotopic analyses of pyrite, Huijiabao Trend, Youjiang Basin, China: Implications for paragenesis and source of sulfur. Economic Geology, 111(2): 331 – 353

Hu RZ, Su WC, Bi XW, Tu GZ and Hofstra AH. 2002. Geology and geochemistry of Carlin-type gold deposits in China. Mineralium Deposita, 37(3 – 4): 378 – 392

Hu RZ, Bi XW, Peng JT, Liu S, Zhong H, Zhao JH and Jiang GH. 2007a. Some problems concerning relationship between Mesozoic-Cenozoic lithospheric extension and uranium metallogenesis in South China. Mineral Deposits, 26(2): 139 – 152 (in Chinese with English abstract)

Hu RZ, Peng JT, Ma DS, Su WC, Shi CH, Bi XW and Tu GC. 2007b. Epoch of large-scale low-temperature mineralizations in southwestern Yangtze massif. Mineral Deposits, 26(6): 583 – 596 (in Chinese with English abstract)

Hu RZ and Zhou MF. 2012. Multiple Mesozoic mineralization events in South China: An introduction to the thematic issue. Mineralium Deposita, 47(6): 579 – 588

Huang YQ and Cui YQ. 2001. The relationship between magmatic rocks and gold mineralization of Mingshan gold deposit of Lingyun, Guangxi. Guangxi Geology, 14(4): 22 – 28 (in Chinese with English abstract)

Johnson CL, Dilles JH, Kent AJR, Farmer LP, Henry CD and Ressel MW. 2015. Petrology and geochemistry of the Emigrant Pass volcanics, Nevada: Implications for a magmatic-hydrothermal origin of the Carlin gold deposits. In: Pennell and Garside (eds.). New Concepts and Discoveries. Lancaster, USA: DEStech Publications, Inc: 391 – 408

Kesler SE, Riciputi LC and Ye ZJ. 2005. Evidence for a magmatic origin for Carlin-type gold deposits: Isotopic composition of sulfur in the Betze-Post-Screamer Deposit, Nevada, USA. Mineralium Deposita, 40(2): 127 – 136

Lai CK, Meffre S, Crawford AJ, Zaw K, Xue CD and Halpin JA. 2014. The western Ailaoshan volcanic belts and their SE Asia connection: A new tectonic model for the Eastern Indochina Block. Gondwana Research, 26(1): 52 – 74

Li SR, Wang DH, Liang T, Qu WJ and Ying LJ. 2008. Metallogenic epochs of the Damingshan tungsten deposit in Guangxi and its prospecting potential. Acta Geologica Sinica, 82(7): 873 – 879 (in Chinese with English abstract)

Li YQ, Pang BC, Yang F, Zhang DW, Zeng QF, Liu X and Jiang XH. 2014. Geochemical characteristics and metallogenic significance of quart porphyry in Liaotun gold deposit, Bama County, Guangxi. Geoscience, 28(6): 1138 – 1150 (in Chinese with English abstract)

Li ZX and Li XH. 2007. Formation of the 1300-km-wide intracontinental orogen and postorogenic magmatic province in Mesozoic South China: A flat-slab subduction model. Geology, 35(2): 179 – 182

Li ZX, Li XH, Chung SL, Lo CH, Xu XS and Li WX. 2012. Magmatic switch-on and switch-off along the South China continental margin since the Permian: Transition from an Andean-type to a Western Pacific-type plate boundary. Tectonophysics, 532 – 535: 271 – 290

Liu HC, Wang YJ, Cawood PA, Fan WM, Cai YF and Xing XW. 2015. Record of Tethyan ocean closure and Indosinian collision along the Ailaoshan suture zone (SW China). Gondwana Research, 27(3): 1292 – 1306

Liu JM, Ye J, Ying HL, Liu JJ, Zheng MH and Gu XX. 2002. Sediment-hosted micro-disseminated gold mineralization constrained by basin paleo-topographic highs in the Youjiang basin, South China. Journal of Asian Earth Sciences, 20(5): 517 – 533

Liu JZ, Deng YM, Liu CQ, Zhang XC and Xia Y. 2006. Metallogenic conditions and model of the superlarge Shuiyindong stratabound gold deposit in Zhenfeng County, Guizhou Province. Geology in China, 33(1): 169 – 177 (in Chinese with English abstract)

Liu S, Su WC, Hu RZ, Feng CX, Gao S, Coulson IM, Wang T, Feng GY, Tao Y and Xia Y. 2010c. Geochronological and geochemical constraints on the petrogenesis of alkaline ultramafic dykes from Southwest Guizhou Province, SW China. Lithos, 114(1 – 2): 253 – 264

Liu YS, Gao S, Hu ZC, Gao CG, Zong KQ and Wang DB. 2010a. Continental and oceanic crust recycling-induced melt-peridotite interactions in the Trans-North China Orogen: U-Pb dating, Hf isotopes and trace elements in zircons from mantle xenoliths. Journal of Petrology, 51(1 – 2): 537 – 571

Liu YS, Hu ZC, Zong KQ, Gao CG, Gao S, Xu J and Chen HH. 2010b. Reappraisement and refinement of zircon U-Pb isotope and trace element analyses by LA-ICP-MS. Chinese Science Bulletin, 55(15): 1535 – 1546

Ludwig KR. 2009. SQUID2: A User's Manual, rev. 12 Apr, 2009.

Berkeley, CA: Berkeley Geochronology Center Special Publication, 5: 1 – 110

Ludwig KR. 2012. Isoplot 3. 75: A Geochronological Toolkit for Microsoft Excel. Berkeley, CA: Berkeley Geochronology Center Special Publication, 5: 75

Mao JW, Xie GQ, Li XF, Zhang CQ and Mei YX. 2004. Mesozoic large scale mineralization and multiple lithospheric extension in South China. Earth Science Frontiers, 11(1): 45 – 55 (in Chinese with English abstract)

Mao JW, Cheng YB, Chen MH and Pirajno F. 2013. Major types and time-space distribution of Mesozoic ore deposits in South China and their geodynamic settings. Mineralium Deposita, 48(3): 267 – 294

Muntean JL, Cline JS, Simon AC and Longo AA. 2011. Magmatic-hydrothermal origin of Nevada's Carlin-type gold deposits. Nature Geosciences, 4(2): 122 – 127

Ovtcharova M, Bucher H, Schaltegger U, Galfetti T, Brayard A and Guex J. 2006. New Early to Middle Triassic U-Pb ages from South China: Calibration with ammonoid biochronozones and implications for the timing of the Triassic biotic recovery. Earth and Planetary Science Letters, 243(3 – 4): 463 – 475

Pang BC, Xiao H, Fu W, Zhang QW and Chen HY. 2014. Microfabric and composition of hydrothermal minerals from the Mingshan Carlin gold deposit in northwestern Guangxi and their implication for ore-forming process. Journal of Jilin University (Earth Science Edition), 44(1): 105 – 119 (in Chinese with English abstract)

Pereira MF, Chichorro M, Solá AR, Silva JB, Sánchez-García T and Bellido F. 2011. Tracing the Cadomian magmatism with detrital/inherited zircon ages by in-situ U-Pb SHRIMP geochronology (Ossa-Morena Zone, SW Iberian Massif). Lithos, 123(1 – 4): 204 – 217

Peters SG, Huang JZ, Li ZP and Jing CG. 2007. Sedimentary rock-hosted Au deposits of the Dian-Qian-Gui area, Guizhou, and Yunnan provinces, and Guangxi District, China. Ore Geology Reviews, 31(1 – 4): 170 – 204

Qin XF, Wang ZQ, Zhang YL, Pan LZ, Hu GA and Zhou FS. 2011. Geochronology and geochemistry of Early Mesozoic acid volcanic rocks from Southwest Guangxi: Constraints on tectonic evolution of the southwestern segment of Qinzhou-Hangzhou joint belt. Acta Petrologica Sinica, 27(3): 794 – 808 (in Chinese with English abstract)

Ressel MW, Noble DC, Henry CD and Trudel WS. 2000. Dike-hosted ores of the Beast deposit and the importance of Eocene magmatism in gold mineralization of the Carlin trend, Nevada. Economic Geology, 95(7): 1417 – 1444

Ressel MW and Henry CD. 2006. Igneous geology of the Carlin Trend, Nevada: Development of the Eocene plutonic complex and significance for Carlin-type gold deposits. Economic Geology, 101(2): 347 – 383

Roger F, Maluski H, Lepvrier C, Vu Van T and Paquette JL. 2012. LA-ICPMS zircons U/Pb dating of Permo-Triassic and Cretaceous magmatisms in northern Vietnam: Geodynamical implications. Journal of Asian Earth Sciences, 48: 72 – 82

Schaltegger U. 2007. Hydrothermal zircon. Elements, 3(1): 51 – 79

Slúma J, Košler J, Condon DJ, Crowley JL, Gerdes A, Hanchar JM, Horstwood MSA, Morris GA, Nasdala L, Norberg N, Schaltegger U, Schoene B, Tubrett MN and Whitehouse MJ. 2008. Plešovice zircon: A new natural reference material for U-Pb and Hf isotopic microanalysis. Chemical Geology, 249(1 – 2): 1 – 35

Stern RA and Amelin Y. 2003. Assessment of errors in SIMS zircon U-Pb geochronology using a natural zircon standard and NIST SRM 610 glass. Chemical Geology, 197(1 – 4): 111 – 142

Stern RA, Bodorkos S, Kamo SL, Hickman AH and Corfu F. 2009. Measurement of SIMS instrumental mass fractionation of Pb isotopes during zircon dating. Geostandards and Geoanalytical Research, 33(2): 145 – 168

Su WC, Xia B, Zhang HT, Zhang XC and Hu RZ. 2008. Visible gold in arsenian pyrite at the Shuiyindong Carlin-type gold deposit, Guizhou, China: Implications for the environment and processes of ore formation. Ore Geology Reviews, 33(3 – 4): 667 – 679

Su WC, Heinrich CA, Pettke T, Zhang XC, Hu RZ and Xia B. 2009a. Sediment-hosted gold deposits in Guizhou, China: Products of wall-rock sulfidation by deep crustal fluids. Economic Geology, 104(1): 73 – 93

Su WC, Hu RZ, Xia B, Xia Y and Liu YP. 2009b. Calcite Sm-Nd isochron age of the Shuiyindong Carlin-type gold deposit, Guizhou, China. Chemical Geology, 258(3 – 4): 269 – 274

Su WC, Zhang HT, Hu RZ, Ge X, Xia B, Chen YY and Zhu C. 2012. Mineralogy and geochemistry of gold-bearing arsenian pyrite from the Shuiyindong Carlin-type gold deposit, Guizhou, China: Implications for gold depositional processes. Mineralium Deposita, 47(6): 653 – 662

Thomas WA. 2011. Detrital-zircon geochronology and sedimentary provenance. Lithosphere, 3(4): 304 – 308

Tretbar DR, Arehart GB and Christensen JN. 2000. Dating gold deposition in a Carlin-type gold deposit using Rb/Sr methods on the mineral galkhaite. Geology, 28(10): 947 – 950

Wang BD, Wang LQ, Chen JL, Yin FG, Wang DB, Zhang WP, Chen LK and Liu H. 2014. Triassic three-stage collision in the Paleo-Tethys: Constraints from magmatism in the Jiangda-Deqen-Weixi continental margin arc, SW China. Gondwana Research, 26(2): 475 – 491

Wang DH, Chen YC, Chen W, Sang HQ, Li HQ, Lu YF, Chen KL and Lin ZM. 2004. Dating of the Dachang superlarge tin-polymetallic deposit in Guangxi and its implication for the genesis of the No. 100 orebody. Acta Geologica Sinica (English Edition), 78(2): 452 – 458

Wang LJ, Yu JH, Griffin WL and O'Reilly SY. 2012. Early crustal evolution in the western Yangtze Block: Evidence from U-Pb and Lu-Hf isotopes on detrital zircons from sedimentary rocks. Precambrian Research, 222 – 223: 368-385

Wang YJ, Fan WM, Zhang GW and Zhang YH. 2013. Phanerozoic tectonics of the South China Block: Key observations and controversies. Gondwana Research, 23(4): 1273-1305

Wang ZP. 2013. Genesis and dynamic mechanism of the epithermal ore deposits, SW Guizhou, China: A case study of gold and antimony deposits. Ph. D. Dissertation. Guiyang: Institute of Geochemistry, Chinese Academy of Sciences, 1-150 (in Chinese with English summary)

Wu YB and Zheng YF. 2004. Genesis of zircon and its constraints on the interpretation of U-Pb age. Chinese Science Bulletin, 49(15): 1554 – 1569

Xia Y, Su WC, Zhang XC and Liu JZ. 2012. Geochemistry and Metallogenic model of Carlin-type gold deposits in Southwest Guizhou Province, China. In: Panagiotaras D (ed.). Geochemistry-Earth's System Processes. InTech, 127 – 156

Xu B, Jiang SY, Wang R, Ma L, Zhao KD and Yan X. 2015. Late Cretaceous granites from the giant Dulong Sn-polymetallic ore district in Yunnan Province, South China: Geochronology, geochemistry, mineral chemistry and Nd-Hf isotopic compositions. Lithos, 218: 54 – 72.

Xu YG, Luo ZY, Huang XL, He B, Xiao L, Xie LW and Shi YR. 2008. Zircon U-Pb and Hf isotope constraints on crustal melting associated with the Emeishan mantle plume. Geochimica et Cosmochimica Acta, 72(13): 3084 – 3104

Yang JH, Cawood PA, Du YS, Huang H and Hu LS. 2012a. Detrital record of Indosinian mountain building in SW China: Provenance of the Middle Triassic turbidites in the Youjiang Basin. Tectonophysics, 574 – 575: 105 – 117

Yang JH, Cawood PA, Du YS, Huang H, Huang HW and Tao P. 2012b. Large Igneous Province and magmatic arc sourced Permian-Triassic volcanogenic sediments in China. Sedimentary Geology, 261 – 262: 120 – 131

Yang WB, Niu HC, Shan Q, Sun WD, Zhang H, Li NB, Jiang YH and Yu XY. 2014. Geochemistry of magmatic and hydrothermal zircon from the highly evolved Baerzhe alkaline granite: Implications for Zr-REE-Nb mineralization. Mineralium Deposita, 49(4): 451 – 470

Zhang XC, Spiro B, Halls C, Stanley CJ and Yang KY. 2003. Sediment-

hosted disseminated gold deposits in Southwest Guizhou, PRC: Their geological setting and origin in relation to mineralogical, fluid inclusion, and stable-isotope characteristics. International Geology Review, 45(5): 407 – 470

Zhang XJ and Xiao JF. 2014. Zircon U-Pb geochronology, Hf isotope and geochemistry study of the Late Permian diabases in the Northwest Guangxi Autonomous Region. Bulletin of Mineralogy, Petrology and Geochemistry, 33(2): 163 – 176

Zhou XM, Sun T, Shen WZ, Shu LS and Niu YL. 2006. Petrogenesis of Mesozoic granitoids and volcanic rocks in South China: A response to tectonic evolution. Episodes, 29(1): 26 – 33

Zhu JJ, Hu RZ, Bi XW, Zhong H and Chen H. 2011. Zircon U-Pb ages, Hf-O isotopes and whole-rock Sr-Nd-Pb isotopic geochemistry of granitoids in the Jinshajiang suture zone, SW China: Constraints on petrogenesis and tectonic evolution of the Paleo-Tethys Ocean. Lithos, 126(3 – 4): 248 – 264

Zi JW, Cawood PA, Fan WM, Wang YJ, Tohver E, McCuaig TC and Peng TP. 2012. Triassic collision in the Paleo-Tethys Ocean constrained by volcanic activity in SW China. Lithos, 144 – 145: 145 – 160

附中文参考文献

陈懋弘, 毛景文, 屈文俊, 吴六灵, Uttley PJ, Norman T, 郑建民, 秦运忠. 2007. 贵州贞丰烂泥沟卡林型金矿床含砷黄铁矿 Re-Os 同位素测年及地质意义. 地质论评, 53(3): 371 – 382

陈懋弘, 黄庆文, 胡瑛, 陈振宇, 章伟. 2009. 贵州烂泥沟金矿层状硅酸盐矿物及其 $^{40}Ar/^{39}Ar$ 年代学研究. 矿物学报, 29(3): 353 – 362

陈懋弘, 陆刚, 李新华. 2012. 桂西北地区石英斑岩脉白云母 $^{40}Ar/^{39}Ar$ 年龄及其地质意义. 高校地质学报, 18(1): 106 – 116

陈懋弘, 张延, 蒙有言, 陆刚, 刘苏桥. 2014. 桂西巴马料屯金矿床成矿年代上限的确定——对滇黔桂"金三角"卡林型金矿年代学研究的启示. 矿床地质, 33(1): 1 – 13

杜远生, 黄虎, 杨江海, 黄宏伟, 陶平, 黄志强, 胡丽沙, 谢春霞. 2013. 晚古生代-中三叠世右江盆地的格局和转换. 地质论评, 59(1): 1 – 11

冯佳睿, 毛景文, 裴荣富, 李超. 2011. 滇东南老君山地区印支期成矿事件初探——以新寨锡矿床和南秧田钨矿床为例. 矿床地质, 30(1): 57 – 73

胡瑞忠, 毕献武, 彭建堂, 刘燊, 钟宏, 赵军红, 蒋国豪. 2007a. 华南地区中生代以来岩石圈伸展及其与铀成矿关系研究的若干问题. 矿床地质, 26(2): 139 – 152

胡瑞忠, 彭建堂, 马东升, 苏文超, 施春华, 毕献武, 涂光炽. 2007b. 扬子地块西南缘大面积低温成矿时代. 矿床地质, 26(6): 583 – 596

黄永全, 崔永勤. 2001. 广西凌云县明山金矿床岩浆岩与金矿化关系. 广西地质, 14(4): 22 – 28

李水如, 王登红, 梁婷, 屈文俊, 应立娟. 2008. 广西大明山钨矿区成矿时代及其找矿前景分析. 地质学报, 82(7): 873 – 879

李院强, 庞保成, 杨锋, 张东伟, 曾庆锋, 刘旭, 蒋新红. 2014. 广西巴马料屯金矿石英斑岩地球化学特征及成矿指示意义. 现代地质, 28(6): 1138 – 1150

刘建中, 邓一明, 刘川勤, 张兴春, 夏勇. 2006. 贵州省贞丰县水银洞层控特大型金矿成矿条件与成矿模式. 中国地质, 33(1): 169 – 177

毛景文, 谢桂青, 李晓峰, 张长青, 梅燕雄. 2004. 华南地区中生代大规模成矿作用与岩石圈多阶段伸展. 地学前缘, 11(1): 45 – 55

庞保成, 肖海, 付伟, 张青伟, 陈宏毅. 2014. 桂西北明山卡林型金矿床热液矿物的显微组构与化学成分特征及其对成矿作用的指示. 吉林大学学报(地球科学版), 44(1): 105 – 119

覃小峰, 王宗起, 张英利, 潘罗忠, 胡贵昂, 周府生. 2011. 桂西南早中生代酸性火山岩年代学和地球化学: 对钦-杭结合带西南段构造演化的约束. 岩石学报, 27(3): 794 – 808

王泽鹏. 2013. 贵州省西南部低温矿床成因及动力学机制研究——以金、锑矿床为例. 博士学位论文. 贵阳: 中国科学院地球化学研究所, 1 – 150

吴元保, 郑永飞. 2004. 锆石成因矿物学研究及其对 U-Pb 年龄解释的制约. 科学通报, 49(16): 1589 – 1604

张晓静, 肖加飞. 2014. 桂西北玉凤、巴马晚二叠世辉绿岩年代学、地球化学特征及成因研究. 矿物岩石地球化学通报, 33(2): 163 – 176